Growth of $Al_2O_3/ZrO_2(Y_2O_3)$ eutectic rods by the laser floating zone technique: effect of the rotation

I. de Francisco, R.I. Merino, V.M. Orera, A. Larrea, J.I. Peña*

Instituto de Ciencia de Materiales de Aragón. CSIC-Universidad de Zaragoza, 50018 Zaragoza, Spain

Abstract

The laser floating zone technique has been applied to the growth of $Al_2O_3/ZrO_2(Y_2O_3)$ rods in the eutectic composition to reveal the effect of forced convection induced by rotation on the rod microstructure. A systematic experimental study of this effect has been carried out combining different source rod and/or eutectic rod rotation (0–200 rpm) and travelling speeds (10–1500 mm/h) in an axial thermal gradient close to 6×10^5 C/m. The results indicate that the rotation is useful to achieve a more homogeneous temperature distribution, especially in thick rods but it has a limited effect in the change of the solidification front shape. The forced convection in the floating zone caused by rotation slightly flattens the solidification interface enhancing the homogeneity of the phase distribution across the sample. However, it introduces several new microstructural features like banding and phase coarsening that can deteriorate the mechanical behaviour of the rods. On the other hand, rods above 1.6 mm in diameter cannot be grown without cracks, even with fast eutectic rod rotation. Rotation does not change the pulling rate threshold (50 mm/h) at which the transition from coupled to dendritic and cellular growth morphology takes place.
© 2004 Elsevier Ltd. All rights reserved.

Keywords: Composites; Microstructure; Al_2O_3–ZrO_2; Directionally solidified eutectics

1. Introduction

Melt Growth Composites produced by controlled solidification of systems in the eutectic composition represent an interesting approach to ceramics with good mechanical properties. The microstructure of several eutectic systems has been widely studied in the last decades because of their promising properties. In particular, the $Al_2O_3/ZrO_2(Y_2O_3)$ eutectic system is of special interest due to its high strength over a wide temperature range, creep resistance, toughness, and chemical stability.[1–3] Room temperature flexural strengths above 1 GPa in eutectic fibres and rods are currently obtained.[4–6]

Several groups have obtained eutectic rods and fibres of $Al_2O_3/ZrO_2(Y_2O_3)$ by directional solidification methods.[5–10] To optimise the mechanical strength, the samples should be free of cracks and pores and have a stable microstructure consisting of fine phases homogeneously distributed preferentially forming an interpenetrating network.[5]

Although the melt of this system is very stable and no apparent vaporization losses are observed, obtaining such an optimum microstructure is far from easy and all these conditions are not generally fulfilled. The laser floating zone (LFZ) method is one of the most useful growth techniques since it provides a good control over the shape of the solidification front, which eventually determines the microstructure of the samples. Moreover, the visualization of the molten zone, source rod and sample during the growth provides an exceptional method to correlate rod morphology with processing conditions.

In previous reports we prepared directionally solidified $ZrO_2(Y_2O_3)$–Al_2O_3 eutectics by the LFZ method and analysed the relationships between growth rate, Y_2O_3 content, residual stresses, mechanical properties, microstructure, crystallographic growth directions and orientation relationships.[11–13] It was concluded that the homogeneity of the microstructure and the absence of extraneous flaws, such as pores or bands, were as important as the fineness of the microstructure in determining sample strength.[5] The mechanical properties are also strongly dependent on the Y_2O_3

---

* Corresponding author. Tel.: +34 976 761958; fax: +34 976 761957.
  E-mail address: jipena@unizar.es (J.I. Peña).

content. The eutectic composition with 3 mol.% Y_2O_3 with respect to $(Y_2O_3 + ZrO_2)$ presented the highest RT strength,[4] therefore, this is the composition we have now selected to work with.

The purpose of the present work is to investigate the influence of pull-rate and rotation rates on the microstructure of $Al_2O_3/ZrO_2(Y_2O_3)$ eutectic rods. The optimum growth parameters to achieve eutectic rods with a homogeneous microstructure are discussed.

2. Experimental procedure

Rods were grown with a CO_2 laser ($\lambda = 10.6\,\mu m$) using the LFZ system at the Instituto de Ciencia de Materiales de Aragón (Spain). The detailed floating zone growth procedure has been described elsewhere.[14] Source rods were obtained from Al_2O_3 (99.99%, Aldrich), ZrO_2 (99+%, Alfa) and Y_2O_3 (99.99%, Aldrich) powders. The starting powder materials were milled in a vibratory micro-mill (model MM2000,
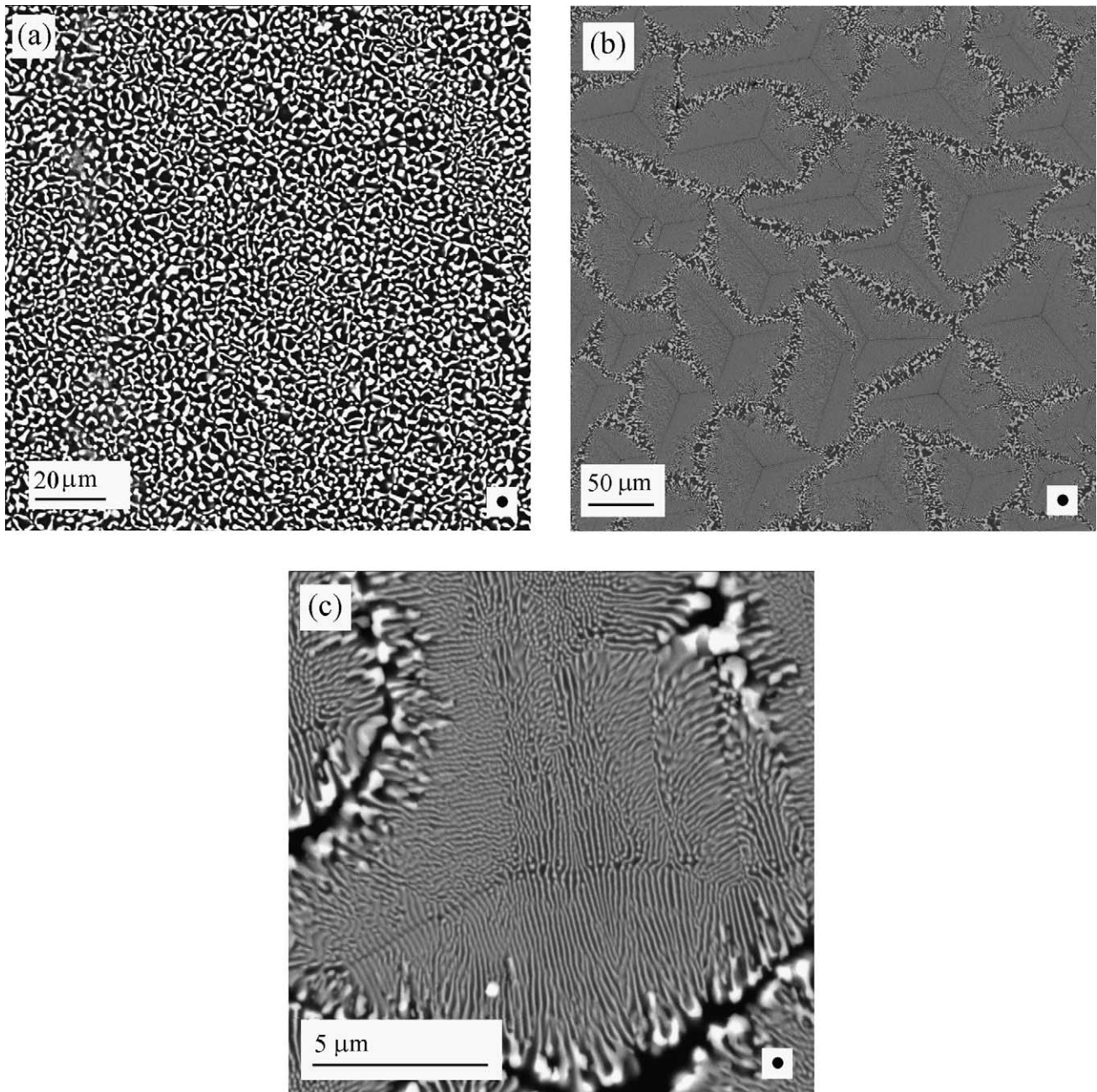

Fig. 1. Microstructures of $Al_2O_3/ZrO_2(Y_2O_3)$ eutectic rods grown by the laser floating zone method. The dark phase is Al_2O_3. SEM images corresponding to transverse cross section of specimens grown at: (a)10 mm/h showing interpenetrating microstructure, (b) 150 mm/h with colony structure and (c) 1500 mm/h showing typical cellular growth. Dots represent the pulling direction perpendicular to the plane.

Resch, Haan, Germany) with acetone using alumina components, fired in air at 1000 °C for 1 h, hand milled in an agate mortar and mixed in the desired composition. The powder was then isostatically pressed for 2 min at 200 MPa and sintered for 12 h at 1250 °C and 1500 °C. The batch composition in mole percent was $62Al_2O_3$–$36.85ZrO_2$–$1.15Y_2O_3$, corresponding to the eutectic composition which has been formulated according to the phase diagram given by Lakiza and Lopato.[15]

Rods in the 1–2 mm diameter range were grown in air with downward pulling at different growth rates from 10 to 2500 mm/h. Identical seed and feed pulling rates without diameter reduction were used in all the cases. The rotation speed of the source rod and/or the grown eutectic rod was varied from 0 to 200 rpm (revolutions per minute).

The length of the molten zone was maintained at about 1.5 times the rod diameter. Pulling rods from low-density ceramic source rods create bubbles in the melt leading to holes and voids in the as-grown rod. To avoid this problem, the rod was remelted in a second step. A first growth step upward at 200 mm/h and counter rotation of 50 rpm was routinely performed to align the system and to get a full density source rod. A polycrystalline seed rod was used to initiate the growth.

Microstructures were observed by optical microscopy and scanning electron microscopy (SEM Jeol, model 6400, Tokyo, Japan) from polished transverse and longitudinal cross-sections of the grown rods. Volume fraction of the phases was estimate by the counting method, with points randomly generated in the image area analysed. Computer analysis of SEM images was used to calculate the lamellar spacing and the solidification front shapes.

3. Results and discussion

3.1. Eutectic microstructures: growth rate dependence

Typical microstructures of Al_2O_3/$ZrO_2(Y_2O_3)$ eutectic rods grown at 10, 150 and 1500 mm/h are shown in Fig. 1. For rods above 1.5 mm in diameter the pull rate has to be limited to less than 1500 mm/h to ensure a complete melting of the zone. At higher velocities no liquid zone could be established, because of the finite thermal conductivity that precludes the melting of the rod centre. Thinner fibres (several hundreds of microns in diameter) could be grown at higher speeds, although our equipment establishes a limit of 3500 mm/h.

At low growth rates, as has been previously reported,[12] the Al_2O_3/$ZrO_2(Y_2O_3)$ eutectic rods solidify with a coupled eutectic microstructure, homogeneous throughout the rod cross-section, and consisting of irregular ZrO_2 lamellae in a continuous Al_2O_3 matrix (Fig. 1a).

When the rate is increased (between 50 and 750 mm/h) a columnar colony microstructure which consists of fi-

bres or lamellae of ZrO_2 embedded in a matrix of Al_2O_3 (Fig. 1b) can be observed. A thick boundary zirconia-rich region (45 vol.% of zirconia) exhibiting a coarser microstructure is formed between the colony grains, as shown in Fig. 1b.

At the highest growth rates the colonies are replaced by a degenerated lamellar microstructure characteristic of cellular growth (Fig. 1c). The onset of the constitutional supercooling leading to morphological instabilities in the solidification interface has been established around 50 mm/h for samples of about 1.5 mm in diameter with a thermal gradient of 6×10^5 °C/m.

Faceted or cellular growth is usually accompanied with the presence of microvoids (around 0.5 μm in size) in the intercellular region. They are produced by the shrinkage due to the difference in density between liquid and solid phase. These microvoids are detrimental to the mechanical properties of the composites. They are more frequently obtained in specimens with the higher yttria content (12 mol.%) because they present wider intercolony boundary regions.

3.2. Shape of the solidification interface

To obtain rods with a homogeneous microstructure formed by fine phases we need a flat and smooth melt-solid interface during growth. In contrast with other compounds,[16,17] in this case the solidification interface can not be observed during growth. The melt is not optically transparent. However, the
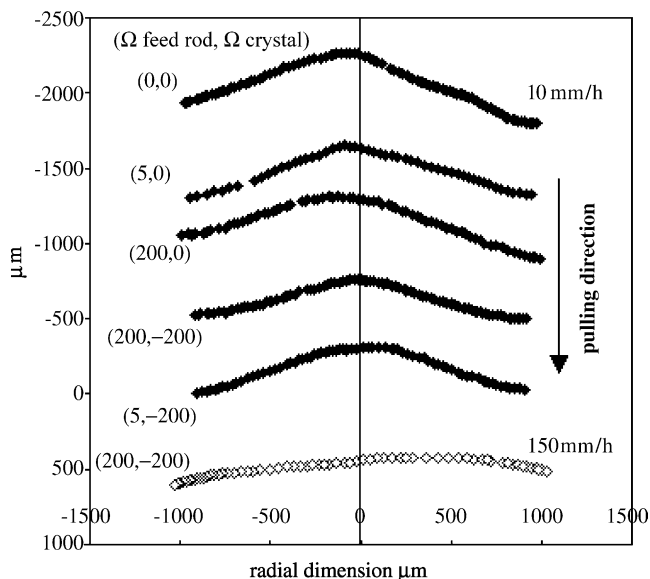

Fig. 2. Shape of the solidification fronts for different processing conditions of source and eutectic rod rotation and pulling rate. The curves were extracted either from the eutectic-frozen melt interface as from the shape of the banding. The numbers in parenthesis are rotation rates of the source and eutectic rod, respectively. The pulling rates are indicated on the right of the curve profile, in mm/h. Curve profiles in filled rhombus correspond to 10 mm/h and curve profiles in empty rhombus correspond to 150 mm/h.

interface can be analysed by observing the formation of defects such as bands in a polished longitudinal cross section of the rods. These defects always follow the solidification front shape. When no such bands are distinguished, the interface between the grown rod and the frozen molten zone is a good image of the solid-melt interface.

In Fig. 2 we represent the solidification profiles for rods grown under different processing conditions obtained using one of the two procedures described above. The solid–liquid interface is always convex towards the melt, as it corresponds to a material with a high absorptivity at the CO_2 laser-radiation wavelength of 10.6 μm.[18]

The interface remains convex towards the melt, even at the highest rotation rates. Without rotation, the profile is convex and irregular. We can observe that even low rotation rates of the source rod are very efficient in homogenising the profile, which becomes more symmetrical, but the effect in overall curvature is less significant. With fast rotation of the source rod only the shape of the interface is less convex and more symmetrical. When fast counter rotation of
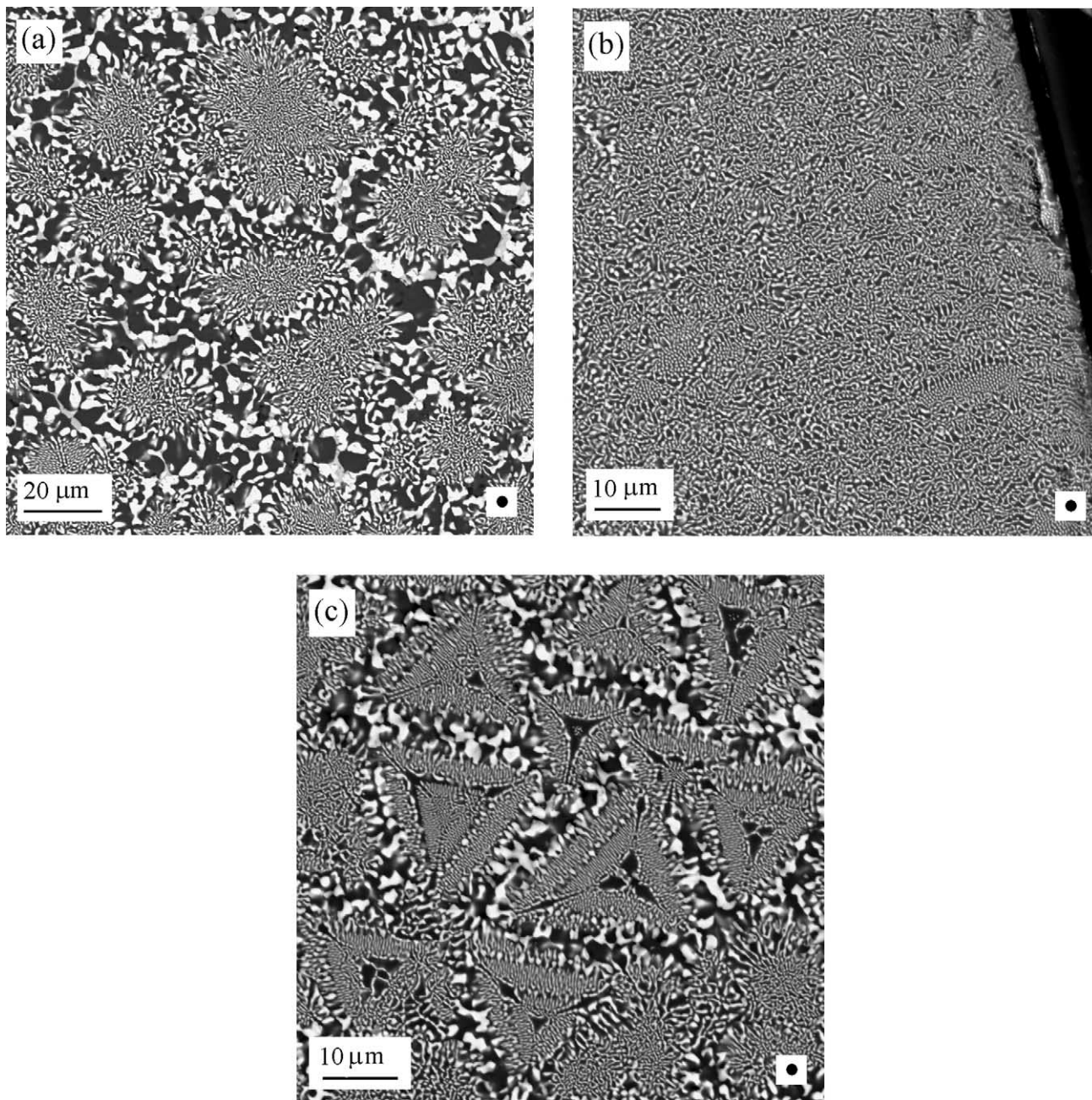

Fig. 3. SEM images showing the microstructure in transverse cross section corresponding to the centre (a) and edge (b) of an $Al_2O_3/ZrO_2(Y_2O_3)$ eutectic rod grown at 100 mm/h without eutectic rod rotation. (c) Grown at the same speed and with a eutectic rod rotation of 200 rpm. Dots represent the pulling direction perpendicular to the plane.

the growing rod is superimposed to that of the source rod rotation the forced convection becomes stronger and the solidification front is then less convex, but not flat. If only the growing rod is rotated a similar effect to counter rotation is observed but the effect in the interface shape is not so strong.

When the pulling rate increases, the front flattens as predicted by Young and Chait.[19] This effect can be due to the increase, as a function of the processing rate, of cooling by radiative heat transfer on the lateral surface of the specimen.

3.3. Effect of source and eutectic rod rotation on microstructure

As has been previously established, when no rotation is used to grow large diameter rods, a relative cooler region arises in the centre of the melt, causing a convex interface and making the thermal gradient higher in the rod periphery than in the centre. To lower the convexity of the interface fast rotation seems to be effective. Since a flat interface should promote microstructure uniformity, vigorous rotation of the
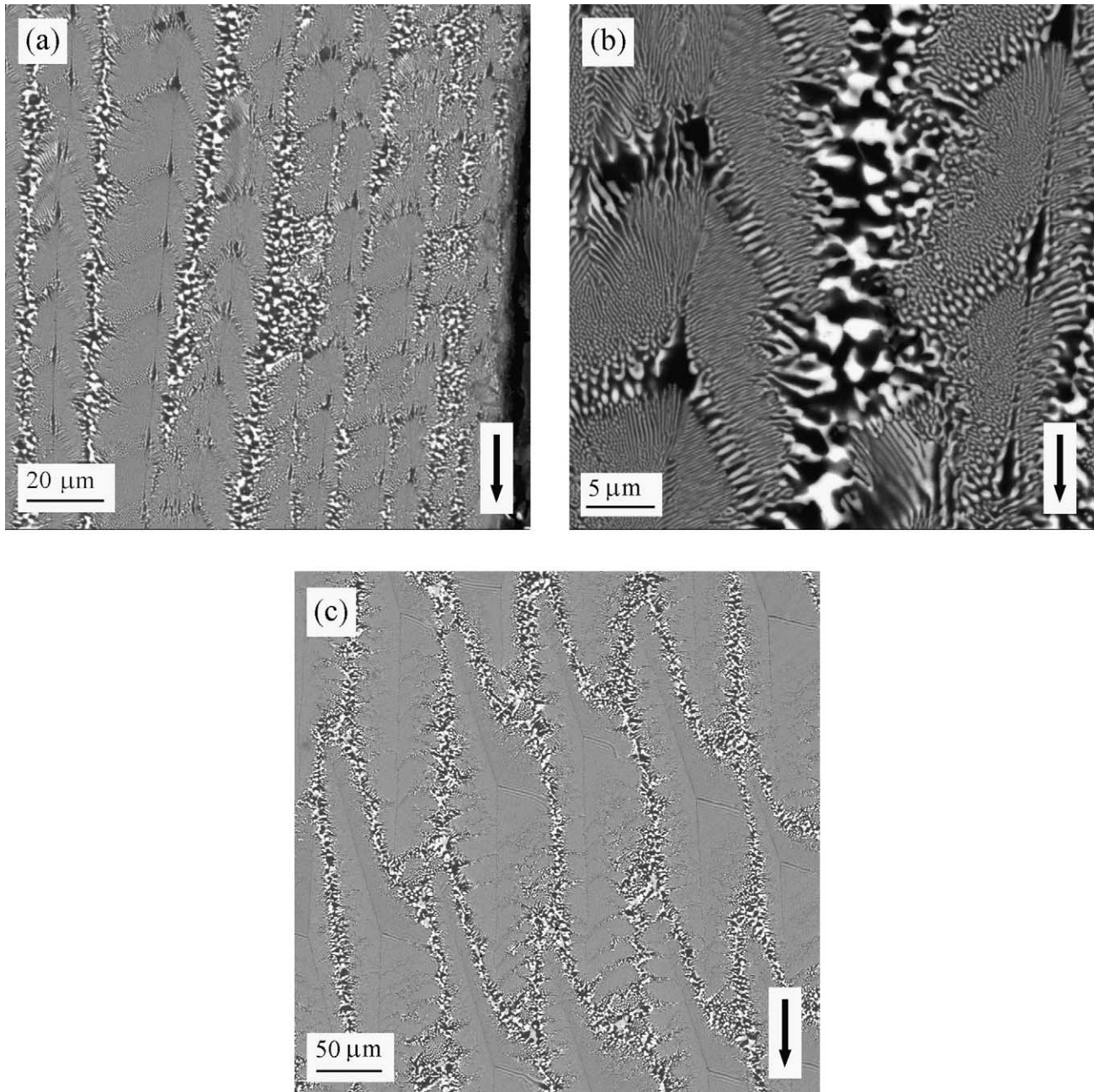

Fig. 4. Longitudinal cross-section of a rod grown at 200 mm/h with a counter rotation of 200 rpm. (a) Colonies in the periphery of the rod showing a periodic continuity rupture, (b) a more detailed image of the colonies and (c) colonies in the centre of the rod, without periodic defects. Arrows represent the pulling direction.
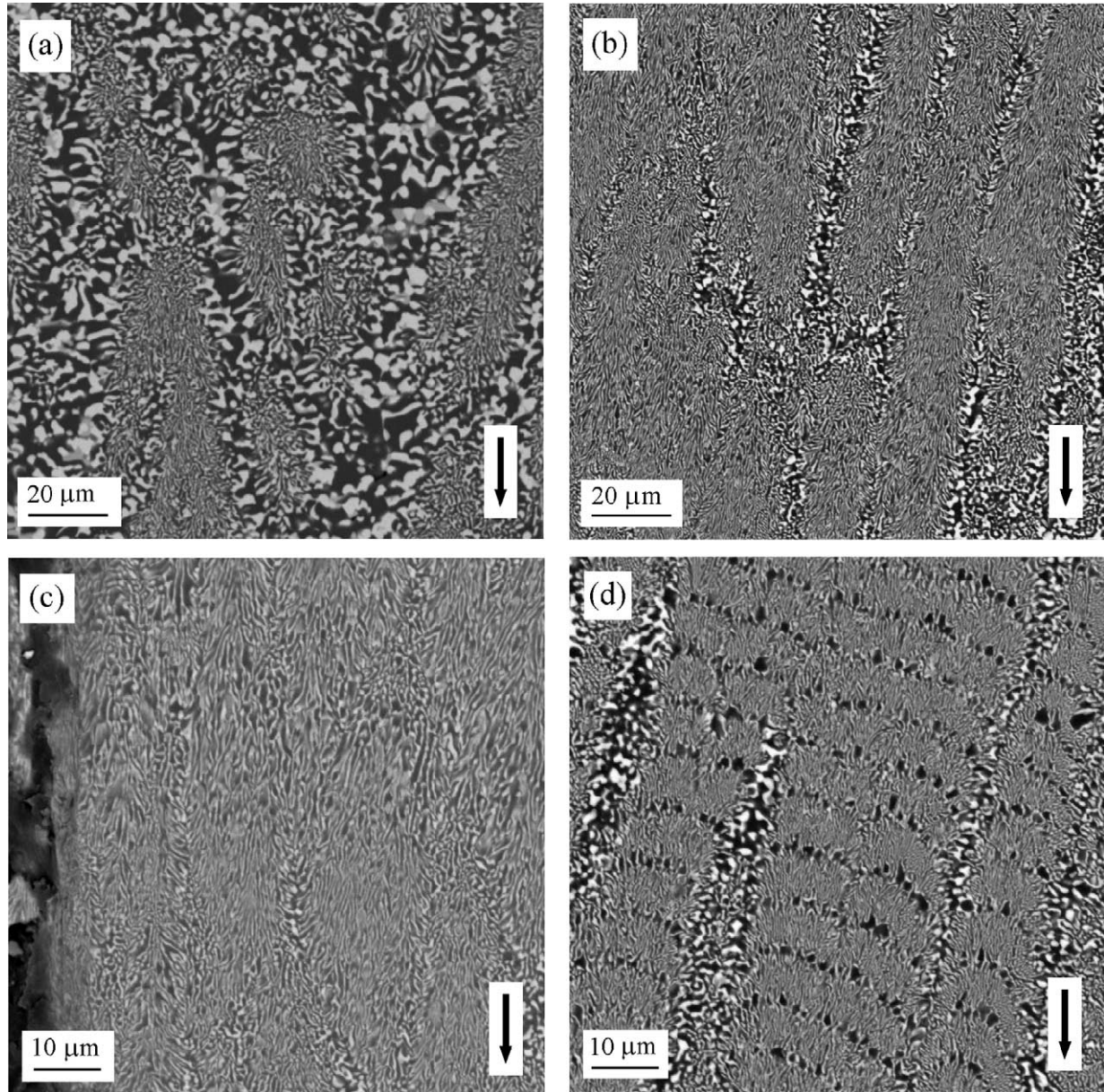
Fig. 5. Longitudinal cross-section of a sample grown at 100 mm/h, without eutectic rod rotation and feed rod rotation of 20 rpm showing the microstructure from the centre to the periphery of the rod (a–c). (d) Outer colonies of a sample grown at 100 mm/h with a eutectic rod rotation of 200 rpm. Arrows represent the pulling direction.

Table 1
Microstructure features corresponding to rods of Al_2O_3/ZrO_2 (Y_2O_3) grown at 10 mm/h under different rotation conditions

Band period (μm)	Rotation (rpm)		Rod diameter	Microstructural features	Mean size of ZrO_2 phase (μm^2)	
	Feed	Crystal			Center	Edge
(30)	0	0	2	Slight bands related to fluctuations. Cracks	2.22	0.94
32	0	5	2.1	Banding associated to eutectic rod rotation	2.50	0.85
(30)	100	0	2	Slight bands related to fluctuations during growth	1.41	0.76
(30)	200	0	2	Slight bands due to fluctuations	2.10	1.29
30	5	−5	1.9	Banding associated to rotation. Cracks	1.69	0.60
	200	−200	1.9	No bands. Cracks	2.46	1.29
30	5	−200	1.9	Slight bands associated to feed rod rotation only seen in the periphery of the rod	2.83	1.96
	5	0	1	No banding. No cracks	2.35	0.98

The band spacing is between parentheses when it is associated with fluctuations.

eutectic rod (200 rpm or more) may be of great help to obtain a more homogenous microstructure. This strategy is recommended for thick rods when the resulting microstructure is radially less uniform.

In Fig. 3a we represent the typical colony microstructure corresponding to the centre of a rod grown at 100 mm/h without eutectic rod rotation. Fig. 3b represents the microstructure corresponding to the border of the rod. It is evident that without rotation there is a microstructure transition from the periphery to the centre of the sample. However, when rotation is applied the colonies extend through the whole sample, as seen in Fig. 3c, corresponding to a rod grown at the same speed, but with eutectic rod rotation (200 rpm).

The same conclusions can be gathered from samples grown at lower rates, either with or without rotation. In this case the microstructure is interpenetrating, rather than colony type, and different phase sizes are observed across the sample, finer in the periphery than in the centre, as described in Table 1. When rotation is applied, this difference is diminished. In light of these observations, it can be asserted that eutectic rod rotation results in a more uniform eutectic, because
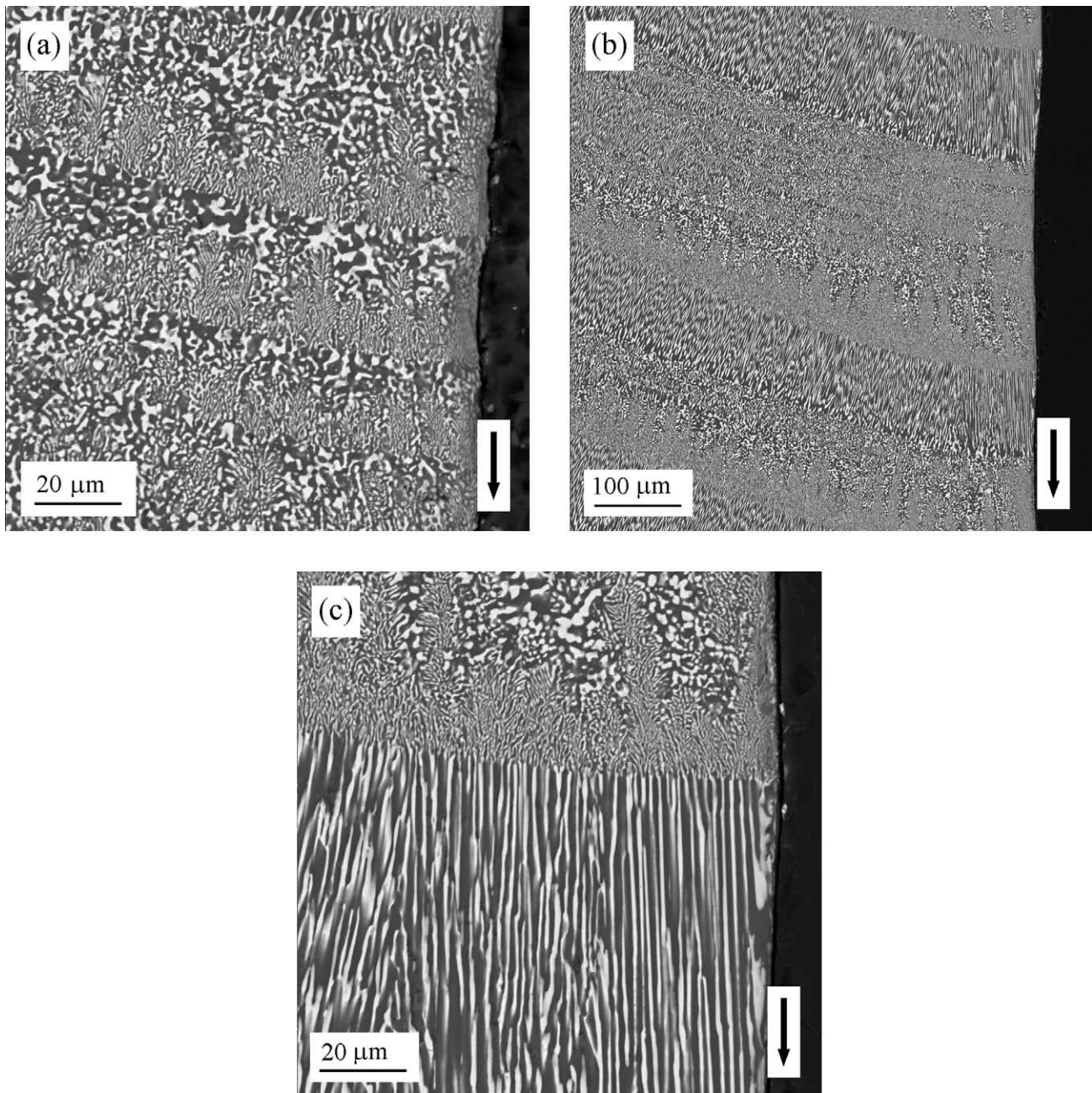

Fig. 6. Longitudinal cross section of a sample grown at 10 mm/h, without eutectic rod rotation, (a) without feed rod rotation, (b) with feed rod rotation of 200 rpm. (c) Detailed view of the microstructure change observed in (b). Arrows represent the pulling direction.

a more homogeneous thermal gradient at the solid/liquid interface is attained.

Despite the fact that rotation of the source rod, eutectic rod or both can achieve a more uniform temperature distribution around the melting zone, a rupture in the continuity of the colonies or segregated phases adopting generally the form of bands are induced in the rod. These defects are very evident when the stirred melt tilts with respect to the growth direction. While the eutectic rod rotates the solidification interface is subjected to a variation in temperature resulting in growth rate changing. For the sake of clarity we will describe the effect of the rotation in band formation separately for rods showing colony or interpenetrating microstructure.

3.3.1. Bands and colony microstructure

Fig. 4a shows the periodic rupture of the ordering of the colonies for a rod grown at 200 mm/h with a counter rotation of 200 rpm. This picture represents a longitudinal cross section of the sample. The periodicity of the defect is about 16 μm corresponding to the solidified length per one turn of the eutectic rod. Fig. 4b shows a closer picture of the colonies. It is remarkable that such banding is rather observed in the outer colonies than in the rod centre, as depicted in Fig. 4c. This assertion has been confirmed in other eutectic rods grown with other growth speed and rotation rates.

The defect disappears when the eutectic rod rotation is eliminated, as can be seen in Fig. 5a–c, corresponding to pictures of colonies taken sequentially from the centre to the periphery of the rod. In this case the sample was grown at 100 mm/h, without eutectic rod rotation and source rod rotation of 20 rpm. At this growth rate, when a eutectic rod rotation of 200 rpm is applied, disruption of the periphery

colonies with a periodicity of about 8 μm is again observed (Fig. 5d). Note the local shape of the growth front, revealed by banding. The front is clearly saw-toothed following the faceted colony nature for 200 mm/h (Fig. 4b), and undulated for 100 mm/h, where the colonies are not faceted (Fig. 5d).

The periodic rupture of the colonies mentioned above is expected to have a minor effect in the mechanical properties of Al_2O_3/ZrO_2 (Y_2O_3) rods, which seems to be mainly controlled by the diameter of the colonies and the width of the colony boundaries.[20]

3.3.2. Bands and interpenetrating microstructure

An interpenetrating microstructure is obtained using low solidification rates. We have also grown different rods varying the rotation speed of source rod and/or eutectic rod. We have observed that this kind of microstructure is very sensitive, not only to rotation, but also to every perturbation occurring during growth (laser power fluctuations, axis hitches, etc). These perturbations can produce periodic segregation or phase coarsening that lead to band formation, which in this case can deteriorate the mechanical properties of the eutectic.

To illustrate the effect of source rod and eutectic rod rotation when an interpenetrating microstructure is obtained, we represent in Fig. 6a the longitudinal cross section of a sample grown at 10 mm/h without any rotation. The image shows the typical interpenetrating microstructure corresponding to a low growth rate, but the presence of periodic bands separated by about 30 microns is rather outstanding. As this defect cannot be assigned to rotation, and it appears each time the sample grows without eutectic rod rotation, we think that it is caused by perturbations present during crystal growth and not related to rotation. The band shape, more evident in the periphery of the rod, reveals the shape of the solidification
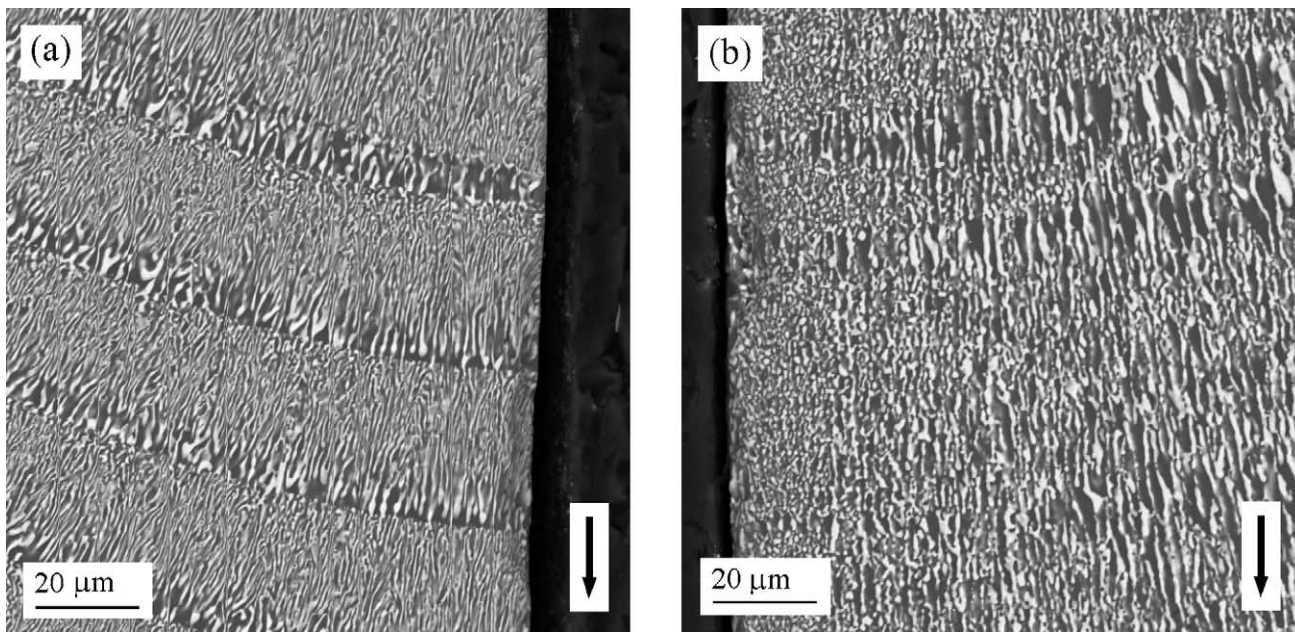

Fig. 7. Longitudinal cross section of a sample grown at 10 mm/h, (a) without feed rod rotation and a eutectic rod rotation of 5 rpm and (b) with a counter rotation of 200 rpm. Arrows represent the pulling direction.

front, convex towards the melt. Interestingly, these problems disappear when some very slow rotation is superposed to the axis displacement.

In the case of slow source rod rotation (5 and 10 rpm) the band distance agrees with the relationship between growth speed and feed rotation. If the source rod rotation is vigorous (100 or 200 rpm) a finer and homogeneous microstructure is developed. Changes from interpenetrating to fibre phase distribution are observed as shown in Fig. 6b. Fig. 6c represents a more detailed view of the zone where the change takes place.

Other experiments have been run to explore the effect of the eutectic rod rotation in the microstructure of the samples. In Fig. 7a we show a longitudinal cross section of a rod grown at 10 mm/h without feed rod rotation. The banding separation of about 30 μm agrees with the eutectic rod rotation of 5 rpm. A counter rotation of 200 rpm provides the most homogeneous sample at this growth rate. The rods show a uniform phase distribution without bands, as is shown in Fig. 7b, because the bands produced by rotation have a separation similar to the phase spacing.

In all of the cases, a magnified view of the bands shows that they consist of a rich Al_2O_3 phase region (vol.% of Al_2O_3 phase is 70 ± 2 compared with the theoretical value of 66.6%).

4. Conclusions

Al_2O_3/ZrO_2 (3 mol.% Y_2O_3) eutectic rods were grown by the LFZ method in a very reproducible way, being its microstructure controlled by the processing conditions. We have grown different rods varying the rotation speed of source rod and/or eutectic rod in order to determine the change in the microstructure of the samples. In summary, we can conclude that:

A transition from coupled to dendrite growth is detected at about 50 mm/h with an axial temperature gradient of 6×10^5 C/m regardless of the rotation speed used.

Counter rotation enhances heat transfer to the centreline of the molten zone. A higher counter rotation speed produces a less convex melt/solid interface.

The lamellar spacing is not uniformly distributed in the radial direction of the solidified sample. The centre of the rod is the region where higher homogeneity is achieved. Fast rotation rates reduce radial temperature gradients ahead of the growth interface, leading to a more uniform phase distribution. However, rotation also causes band formation in rods with an interpenetrating microstructure, or interruption in the continuity of the outer columnar colonies within the colony microstructure.

These periodic defects should be taken into consideration for the mechanical behaviour of the samples. Particularly advantageous is fast counterrotation, in order to prevent perturbations of the interpenetrating microstructure associated to mechanical instabilities of the growth equipment.

References

1. Echigoya, J., Takabayashi, Y. and Suto, H., Hardness and fracture toughness of directionally solidified $Al_2O_3–ZrO_2(Y_2O_3)$ eutectics. *Mater. Sci. Lett.*, 1986, **5**, 153–154.
2. Borodin, V. A., Starotsin, M. Y u. and Yalovets, T. N., Structure and related mechanical properties of shaped eutectic $Al_2O_3–ZrO_2$ (Y_2O_3) composites. *J. Crystal Growth*, 1990, **104**, 148–153.
3. Sayir, A., Farmer, S. C., Dickerson, P. O. and Yun, H. M., High temperature mechanical properties of $Al_2O_3–ZrO_2(Y_2O_3)$ fibers. *Mater. Res. Soc. Symp. Proc.*, 1995, **365**, 21–27.
4. Llorca, J., Pastor, J. Y., Poza, P., Peña, J. I., de Francisco, I., Larrea, A., and Orera, V. M., Influence of the Y_2O_3 content and temperature on the mechanical properties of melt-grown $Al_2O_3–ZrO_2$ eutectics. *J. Am. Ceram. Soc.*, 2004, **87**, 633–639.
5. Pastor, J. Y., Llorca, J., Poza, P., de Francisco, I., Merino, R. I. and Peña, J. I., Mechanical properties of melt-grown $Al_2O_3–ZrO_2(Y_2O_3)$ eutectics with different microstructure. *J. Eur. Ceram. Soc.*, 2005, **25**, 1215–1223.
6. Farmer, S. C., Sayir, A. and Dickerson, P. O., Mechanical and microstructural characterization of directionally-solidified alumina-zirconia eutectic fibers. *In situ Composites Science and Technology*. TMS, Warrendale, PA, USA, 1993, pp. 167–182.
7. Courtright, E. L., Haggerty, J. S. and Sigalovsky, J., Controlling microstructures in $ZrO_2(Y_2O_3)–Al_2O_3$ eutectic fibers. *Ceram. Eng. Sci. Proc.*, 1993, **14**, 671–681.
8. Bates, H. E., EFG growth of alumina-zirconia eutectic fiber. *Ceram. Eng. Sci. Proc.*, 1992, **13**, 190–197.
9. Lee, J. H., Yoshikawa, A., Durbin, S. D., Yoon, D. H., Fukuda, T. and Waku, Y. J., Microstructure of Al_2O_3/ZrO_2 eutectic fibers grown by the micro-pulling down method. *Crystal Growth*, 2001, **222**, 791–796.
10. Famer, S. C. and Sayir, A., Tensile strength and microstructure of $Al_2O_3–ZrO_2$ hypo-eutectic fibres. *Eng. Fracture Mech.*, 2002, **69**, 1015–1024.
11. Harlan, N. R., Merino, R. I., Peña, J. I., Larrea, A., Orera, V. M., González, C., Poza, P. and Llorca, J., Phase distribution and residual stresses in melt-grown $Al_2O_3–ZrO_2(Y_2O_3)$ eutectics. *J. Am. Ceram. Soc.*, 2002, **85**, 2025–2032.
12. Peña, J. I., Merino, R. I., Harlan, N. R., Larrea, A., de la Fuente, G. F. and Orera, V. M., Microstructure of Y_2O_3 doped $Al_2O_3–ZrO_2$ eutectics grown by the laser floating zone method. *J. Eur. Ceram. Soc.*, 2002, **22**, 2595–2602.
13. Merino, R. I., Peña, J. I., Harlan, N. R., de la Fuente, G. F., Larrea, A., Pardo, J. A., Orera, V. M., Pastor, J. Y., Poza, P. and Llorca, J., Phase distribution, residual stresses and mechanical properties of melt growth $Al_2O_3-ZrO_2(Y_2O_3)$ eutectics. *Ceram. Eng. Sci. Proc.*, 2003, **23**, 663–670.
14. Peña, J. I., Merino, R. I., de la Fuente, G. F. and Orera, V. M., Aligned $ZrO_2(c)$-$CaZrO_3$ eutectics grown by the laser floating zone method: electrical and optical properties. *Adv. Mater.*, 1996, **8**, 909–912.

15. Lakiza, S. M. and Lopato, L. M., Stable and metastable phase relations in the system alumina-zirconia-yttria. *J. Am. Ceram. Soc.*, 1997, **80**, 893–902.

16. Lan, C. W., Yang, D. Y., Ting, C. C. and Chen, F. C., A transparent furnace for crystal growth and flow visualization. *J. Crystal Growth*, 1994, **142**, 373–378.

17. Tao, Y. and Kou, S., Flow visualization in floating zone crystal growth-a videotape movie. *J. Crystal growth*, 1994, **137**, 72–76.

18. Tsuiki, H., Temperature distribution near the molten zone in a floating zone imaging furnace: fundamental method of calculation. *J. Crystal Growth*, 1986, **76**, 419–428.

19. Young, G. W. and Chait, A., Steady-state thermal–solutal diffusion in a float zone. *J. Crystal Growth*, 1989, **96**, 65–95.

20. Pastor, J. Y., Poza, P., Llorca, J., Peña, J. I., Merino, R. I. and Orera, V. M., Mechanical properties of directionally solidified Al_2O_3-$ZrO_2(Y_2O_3)$ eutectics. *Mater. Sci. Eng.*, 2001, **A308**, 241–249.